



## PERFORMANCE ASSESSMENT OF LATERALLY-LOADED NORMAL AND HIGH STRENGTH STEEL-REINFORCED DRILLED SHAFTS USING 1-D AND 3-D NUMERICAL METHODS

A. Ganji<sup>(1)</sup>, Q. Li<sup>(2)</sup>, P. Arduino<sup>(3)</sup>, and A. Stuedlein<sup>(4)</sup>

<sup>(1)</sup> Graduate Student, University of Washington, Seattle, WA, USA; [ganjia@u.washington.edu](mailto:ganjia@u.washington.edu)

<sup>(2)</sup> Graduate Student, Oregon State University, Corvallis, OR, USA; [liqiang@onid.oregonstate.edu](mailto:liqiang@onid.oregonstate.edu)

<sup>(3)</sup> Professor, University of Washington, Seattle, WA, USA; [parduino@uw.edu](mailto:parduino@uw.edu)

<sup>(4)</sup> Associate Professor, Oregon State University, Corvallis, OR, USA; [armin.stuedlein@oregonstate.edu](mailto:armin.stuedlein@oregonstate.edu)

### **Abstract**

The use of high strength steel reinforcement bar in drilled shaft construction is not common in transportation infrastructure applications due to the lack of familiarity with the materials, performance characteristics, and the suitability of existing methods for the assessment of performance. For example, traditional 1-D modeling approaches may not adequately capture the beneficial effect of concrete confinement, related to the presence of stiffer flexural and shear reinforcement distributed throughout the steel reinforcement cage, on the global strength and stiffness to lateral loads. This effect is critical to evaluate, as the use of high strength bar necessarily leads to less area of steel in a drilled shaft foundation. However, the use of high strength bar would yield less congested steel cages and development of fewer construction defects as a result, and would also be quicker to construct, and easier to handle. Studies illustrating the suitability of traditional approaches for modeling the performance of high strength steel-reinforced drilled shafts could assist practitioners in allowing such materials in their specifications. This paper describes the results of comparative numerical studies performed to evaluate the performance of 1-D  $p$ - $y$  methods to predict the lateral load response of drilled shafts reinforced with normal (60 ksi) and high strength (80 ksi) steel reinforcement. The performance of 1-D methods is evaluated using sophisticated 3-D methods that account for the distribution of steel within the shaft cross-section and its effect on concrete confinement, as well as scale or diameter effects on the lateral soil response. These studies indicate that the 1-D methods are sufficiently accurate for use in design of shafts with high strength reinforcement, but remain susceptible to scale effects.

*Keywords: shaft analysis, lateral loads, numerical analysis, finite elements*



## 1.0 Introduction

Drilled shafts provide significant geotechnical resistance for support of highway bridges, and are used throughout the States of Oregon and Washington to meet their structural foundation requirements. Due to changes in construction methods and poor near-surface soils, the use of permanent steel casing for drilled shaft installation has increased. However, geotechnical design models for axial and lateral resistance of drilled shafts are largely based on soil-concrete interfaces, not soil-steel interfaces associated with large diameter steel casing. Owing to the improved understanding of our regional seismic hazards, the amount of steel reinforcement used in drilled shaft construction has increased over the past several decades, creating a new construction concern for engineers: the greater steel area results in a reduced clearance between adjacent reinforcement bars in the steel cage, such that concrete has an increased difficulty in penetrating the cage and likelihood for voids and defects within the shaft, which can lead to poor structural and geotechnical performance. The use of high-strength reinforcement steel can lead to improved clearance within the steel cage, mitigating concreting issues. The use of steel casing and the amount of steel area control the axial and lateral resistance of the shaft. However, depending on the method of construction, the steel casing may result in reduced axial load transfer to the surrounding soil. Thus existing analytical approaches need to be evaluated for modern construction methods, and new approaches developed if necessary to ensure desired performance criteria are met. For this purpose, and as a first step, numerical methods are evaluated for their capabilities to capture the response of shafts to axial and lateral loads.

The research presented in this paper is part of a larger research project that is set within a collaborative framework including ODOT, WSDOT, PacTrans, and the West Coast Chapter of the Association of Drilled Shaft Contractors (WCC-ADSC). The objectives of the overall project are to study the impact of steel casing and high-strength steel reinforcement on the axial and lateral behavior of full-scale drilled shaft foundation elements and to evaluate the appropriateness of existing design procedures.

## 2.0 Overview of Modeling Approach

This project aims to evaluate the performance of drilled shafts with high strength reinforcement and casing. This paper describes the development of 1-D conventional ( $p$ - $y$  method) and 3-D finite element models using the OpenSees framework. The purpose of this study is to explore the capability of OpenSees to capture the 3-D response of deep foundations subjected to lateral loads. For this purpose, 1-D simulations are compared to results from 3-D models.

For consistency, the same shaft geometry and soil conditions are used in the evaluation of each numerical approach. The sections include a baseline shaft, shaft with high-strength steel, shaft with casing and shaft with casing and internal reinforcement and correspond to those constructed at a test site.

The benefit of using OpenSees is that in addition to 1-D models, OpenSees also provides the possibility of generating 3-D finite element models representative of the same 1-D problems; in this case soil shaft interaction models. Although 3-D finite element analyses are expensive in terms of time and computational cost, this study uses them to validate results from 1-D conventional analyses.

The Open System for Earthquake Engineering Simulation (OpenSees) is an open source and object-oriented framework developed at the Pacific Earthquake Engineering Research Center (PEER) at the University of California, Berkeley (download at <http://opensees.berkeley.edu/>). OpenSees is widely used for the nonlinear analysis of geotechnical and structural systems. OpenSees has a large library of constitutive models for steel, concrete, sand, clay and other materials in both uniaxial and multi-dimensional spaces, elements, sections, and loading patterns. Its main application is for the analysis of structural and geotechnical systems subjected to static and dynamic loads; in particular earthquake loads.

## 3.0 Soil Properties and Shaft Section

The site selected for this study is located at Oregon State University's geotechnical site. The site has been used for geotechnical full-scale tests for over twenty years. Several surface investigations and site exploration

programs are available and were used to estimate the mechanical properties of the soil to a depth of 60 feet (18.3 m). Using this information, three different soil layers are identified and are shown in Figure 1. The ground water level is assumed at 7 feet (2.1 m) below the ground surface. This level represents the conditions during the summer when the future full tests will be performed. A summary of the relevant soil data available to perform 1-D and 3-D numerical simulations is presented in Figure 1(a) and Table 1.

Table 1 Soil properties

Soil Profile	Effective Unit Weight ( $kN/m^3$ )	Undrained Cohesion ( $kPa$ )	Strain Factor, $\epsilon_{50}$	Friction Angle ( $degree$ )	Soil Modulus Parameter, $k$ ( $MN/m^3$ )
Clayey silt (Upper and Lower Cohesive)	8.26	62.2	0.007	-	135.7
Sand	10.62	-	-	40	40.7
Blue Gray Clay	7.48	167.6	0.005	-	271.4

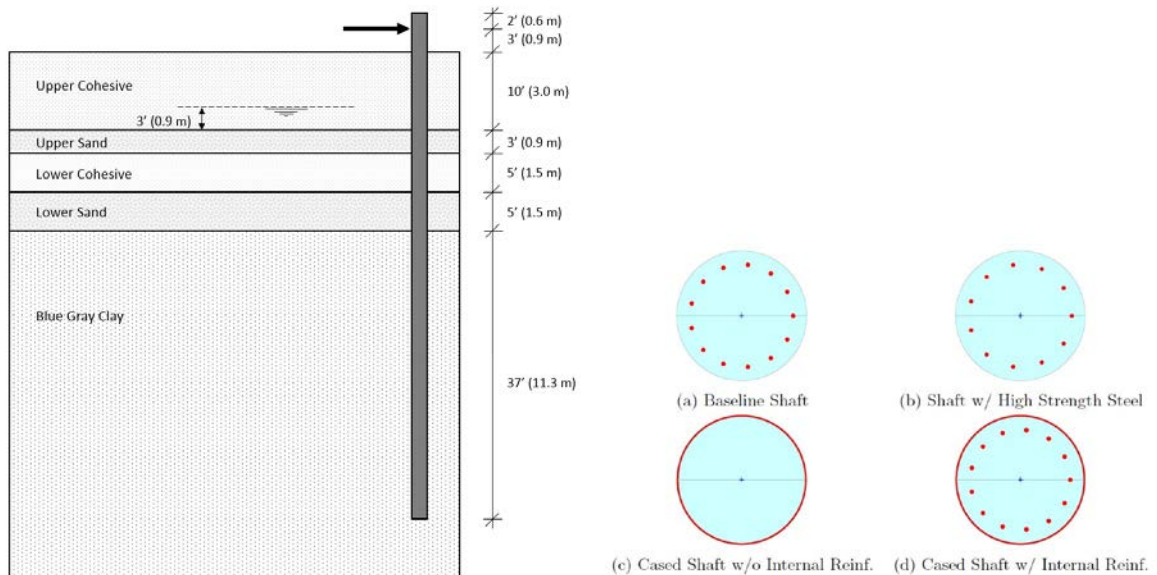


Fig. 1 – Geometry considered: (a) soil profile and (b) shaft sections

In this study, four reinforced concrete drilled shafts sections are considered. For all shafts, total and embedded lengths are 65 and 60 feet (18.3 and 19.8 meters). Lateral loads are applied 2 feet (0.6 meter) below the head of each shaft. The section diameter for all cases is 36 inches (914.4 mm). Each section is different in terms of reinforcement. The first section, referred in this study as baseline shaft or MIR (Mild Internal Steel Reinforcement) is a common concrete shaft reinforced with 13 mild bars (strength of 420 MPa and No. 11 rebar size). The second section referred as shaft with high-strength steel or HSIR (High-Strength Internal Reinforcement) is the same as the baseline shaft except having 12 high-strength bars (strength of 550 MPa and No. 10 rebar size). The third section is simply a concrete-filled steel tube (CFT) without internal reinforcement or CNIR (Cased, No Internal Reinforcement), and the fourth section is a CFT with the same bars as the baseline shaft referred as CIR (Cased, mild Internal Reinforcement). Note that the thickness and strength of the casing for the last two sections are 0.5 inch (12.7 mm) and 50 ksi (350 MPa) respectively. The sections are schematically shown in Figure 1(b).



The concrete properties are the same for all sections. The selected compression strength is 4 ksf (28 MPa), Young’s modulus is 3605 ksi (25 GPa), modulus of rupture of concrete is estimated at 0.4743 ksi (3.3 MPa) and the tensile strain at fracture is  $1.15E^{-4}$ . The geometry of each shaft is summarized in Table 2.

Table 2 Summary of shafts properties used in OpenSees

Shaft name	Diameter m (in)	Total Length m (ft.)	Embedded Length m (ft.)	Casing Wall Thickness mm (in)	Percentage of Internal and External Steel
Mild Internal Steel Reinforcement (MIR)	0.9 (36)	19.8 (65)	18.3 (60)	0	2 %
High-strength Internal Reinforcement (HSIR)	0.9 (36)	19.8 (65)	18.3 (60)	0	1.5 %
Cased, No Internal Reinforcement (CNIR)	0.9 (36)	19.8 (65)	18.3 (60)	12.7 (0.5)	5.5 %
Cased, Mild Internal Reinforcement (CIR)	0.9 (36)	19.8 (65)	18.3 (60)	12.7 (0.5)	7.5 %

To define structural (shaft) elements, several options are available in OpenSees. Among them, displacement-based elements are commonly used (element *dispBeamColumn*) in OpenSees. This element considers plasticity along the element and is appropriate to characterize the nonlinear response of a shaft.

#### 4.0 Section Analysis

The first step in creating an OpenSees model for a soil-shaft interaction system is to define the shaft section and obtain a moment-curvature relationship representative of the nonlinear structural response to bending. For this purpose the concept of a fiber section, available in OpenSees, is used. Fiber sections consist of numerous uniaxial fibers distributed in radial and angular divisions.

The fibers are uniaxial, can be used to represent steel and concrete, and provide the correct one dimensional longitudinal nonlinear constitutive behavior for each material. The fiber section concept assumes there is no slip between fibers and that plane sections remain plane. In OpenSees, to define steel fibers, the *Steel01* uniaxial constitutive model is used. To capture the concrete response, the confinement condition must be considered since it strongly affects sectional properties. Confined concrete sections not only show higher compression resistance, but also higher ductility. To define concrete fibers in OpenSees, the *concrete01* and *concrete02* uniaxial constitutive models are used. The resulting moment-curvature curves are shown in Figure 2 illustrating the result of this approach.

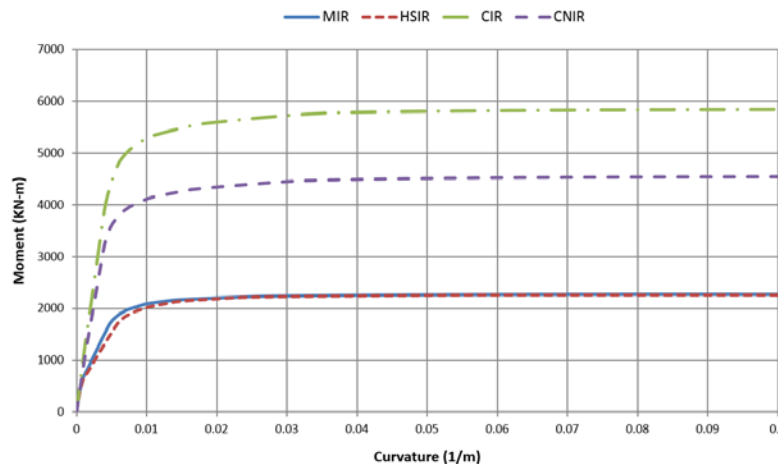


Fig. 2 - Moment-curvature relationships extracted from OpenSees model



The figure shows that sections MIR and HSIR perform similarly in bending. It also shows that using casing increases the moment capacity of the section considerably. As inferred from Figure 2 and Table 2, comparing sections reinforced by rebar (MIR and HSIR) and sections reinforced by casing (CNIR and CIR) it is clear that casing increases the ductility significantly. As the ductility and the moment capacity increase, the piles are able to store more energy in lateral loading and plastic deformation.

## 5.0 1-D Conventional Finite Element Analysis

Soil-pile interaction is a complicated physical problem to represent numerically. In theory, to capture details and complexities of soil-pile interaction systems a full 3-D finite element model must be used. In practice, Beam on Nonlinear Winkler Foundation (BNWF) models are commonly used, remarkably decreasing the computational cost, time and complexity. This approach greatly simplifies a complicated 3-D model into a simple 1-D model if assumptions used to extract the 1D differential equation are satisfied. In this approach the pile is represented by beam elements and the soil is represented by springs oriented at different directions. For the site under consideration in this study, the soil is reported homogenous and the shaft deformation is small compared to the shaft length. Therefore, the BNWF approach is applicable for both axial and lateral loading.

In 1-D conventional finite element methods, the axial and lateral deformations are decoupled such that axial and lateral loads are applied, and deformations calculated, independently. In axial loading, as shown in Figure 3, there are two different components of resistance to consider including: side resistance, modeled using  $t$ - $z$  springs along the sides of the shaft, and tip resistance modeled using a  $q$ - $z$  spring at the end of the shaft. The soil lateral resistance is modeled using  $p$ - $y$  springs representing the soil resistance to lateral loads.

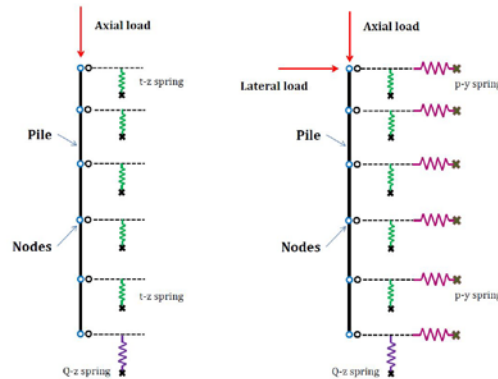


Fig. 3 - Schematic models for 1D analysis in vertical and lateral loading

Different theories have been developed to represent  $t$ - $z$ ,  $q$ - $z$  and  $p$ - $y$  springs, and different implementations are available in different codes. OpenSees uses uniaxial materials for sands and clays to characterize these springs. A brief note on the parameter required to define  $t$ - $z$ ,  $q$ - $z$  and  $p$ - $y$  curves in OpenSees is included here. A complete step-by-step procedure is described in [1].

### 5.1 Axial Loading

The vertical resistance of the soil-shaft system is simulated using  $t$ - $z$  and  $q$ - $z$  springs. OpenSees provides  $t$ - $z$  and  $q$ - $z$  uniaxial material models for this purpose. To define  $t$ - $z$  springs in OpenSees, two parameters must be determined and assigned to the material models, including: the ultimate capacity of the  $t$ - $z$  spring,  $t_u$ , and the vertical displacement at which 50% of  $t_u$  is mobilized in monotonic loading,  $z_{50}$ .

The ultimate vertical soil resistance,  $t_u$ , can be obtained following Kulhawy (1991) [2] equation for cohesionless soils in terms of effective vertical stress,  $\sigma'_v$ , at-rest lateral earth pressure coefficient,  $K_0$ , and interface friction angle between shaft and soil,  $\delta$ . To find  $z_{50}$ , different approaches are used for sand and clay. For sand, the procedure proposed by Mosher and Dawkins (2000) is used. For cohesive soils, the procedure



proposed by Reese and O'Neill (1988) [3] is used. Following this approach, Boulanger et al. (1999) [4] implemented the *TzSimple1* material in OpenSees.

To define *q-z* springs, to be applied at the shaft toe, the ultimate capacity at the tip,  $Q_u$ , can be expressed in terms of ultimate bearing resistance expressions for clays and sands and an hyperbolic expression is defined in terms of a critical toe deflection  $z_{50}$ , the toe deflection at which 50% of the ultimate resistance is mobilized in monotonic loading. Following this approach, Boulanger et al. (1999) [4] implemented the *QzSimple1* material in OpenSees.

Using these OpenSees modeling elements Figure 4 presents results of axial analyses for sections MIR/HSIR and CIR/CNIR.

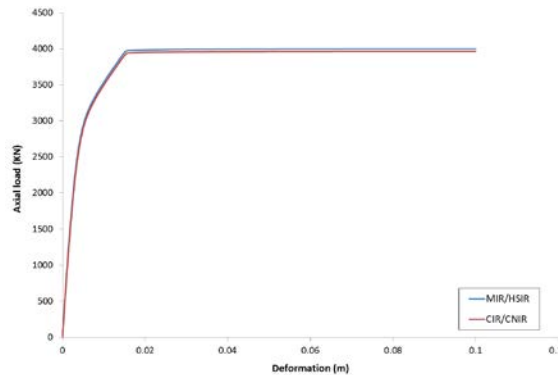


Fig. 4 - Axial load capacity of shafts

As shown in Figure 4 and presented in Table 3, axial capacity of sections MIR and HSIR is 4000 kN, while axial capacity of sections CNIR and CIR is 3963 kN. The difference is originated from interface friction angle which is 40 degrees for the sections without casing and 32 degrees for the cased sections. For both types, the tip resistance is the same and equal to 990 kN.

Table 3 Axial load capacity of each section

Sections	MIR	HSIR	CNIR	CIR
Shaft Resistance (kN)	3010	3010	2973	2973
Toe Resistance (kN)	990	990	990	990
Total Axial Resistance (kN)	4000	4000	3963	3963

## 5.2 Lateral Loading

Lateral load shaft analysis is performed using a similar approach as for axially-loaded shafts but in addition to the axial springs, lateral uniaxial springs are necessary. The lateral springs are referred as *p-y* springs. To model *p-y* springs in OpenSees, the uniaxial material *PySimple1* is used. *PySimple1* is based on the equation proposed by Boulanger et al. (1999) [4]. The nonlinear *p-y* curve is defined using elastic and plastic force-deformation relationships and includes a gap component. Main parameters to define the *p-y* curve include soil type (clay or sand), the ultimate capacity of the *p-y* curve,  $p_u$ , and the displacement at which 50% of  $p_u$  is mobilized in monotonic loading. OpenSees provides a response "soil type 1", which captures the *p-y* backbone curve proposed by Matlock (1970) [5] for soft clays. "Soil type 2" uses the API (1993) [6] relationship for sand.

Having expressions and parameters for  $p_u$  and displacement at 50%  $p_u$ , equal to  $y_{50}$  allows the definition of *p-y* springs *PySimple1* in OpenSees. Figure 5 shows the lateral load-displacement response for sections MIR, HSIR, CNIR and CIR as obtained using an OpenSees model. As can be seen in the figure, the lateral resistance of sections MIR and HSIR are similar, while the cased sections CNIR and CIR show significantly higher resistance. In addition to the load-displacement relationship presented in Figure 5,



deformation, shear force and bending moment versus depth are necessary to properly evaluate the shaft response. As an example, Figure 6 displays deflection, shear force and bending moment versus depth for section CNIR as calculated by OpenSees using the 1D models. Results for other sections are presented later in a comparison with results from 3D simulations.

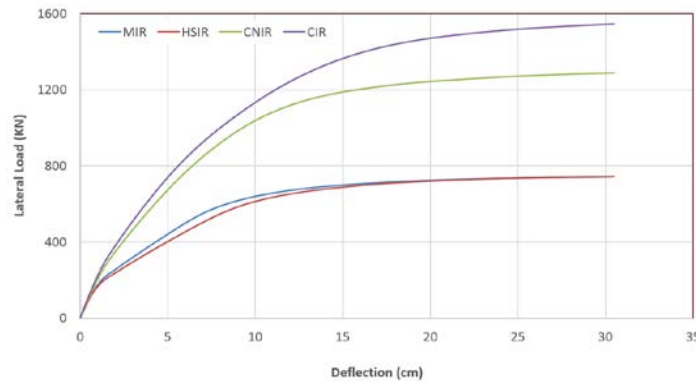


Fig. 5 - Lateral load-displacement at the top of the shaft

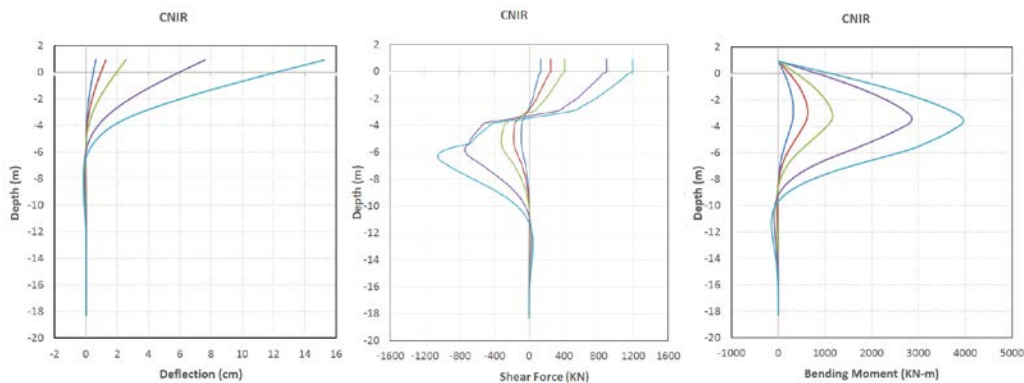


Fig. 6 - 1D OpenSees Model. Deflection, shear force and bending moment versus depth at selected imposed displacements at the top of the shaft for CNIR section

Based on these 1-D models, the lateral capacities of the shafts are predicted roughly as 745, 743, 1289 and 1546 kN for sections MIR, HSIR, CNIR and CIR respectively. The results show that using casing around the shaft (MIR) adds 107% extra lateral strength to section (CIR). Also, using casing without the internal reinforcement increases the lateral resistance of the shaft by 73%.

### 6.0 3-D Finite Element Analysis

As mentioned in the previous section, 3-D finite element modeling is considered the most accurate way for simulating an embedded shaft subjected to lateral loading. 3-D FEM models equip researchers with more tools to estimate the real behavior of shafts. OpenSees provides a framework in which materials, elements, and other components necessary for modeling soil-shaft interaction within a 3-D finite element environment are possible. To enable efficient modeling in OpenSees, the GiD program (<http://gid.cimne.upc.es/>) is used as a pre- and post-processor.

The procedure for creating a 3-D finite element model of a shaft subjected to lateral loading requires three general steps: a) creating a 3-D model of the foundation system, b) defining nodes, nodal fixities, soil elements, and shaft elements taking advantage of symmetries when possible to reduce the computational cost and c) assigning material properties based on given field and laboratory data.

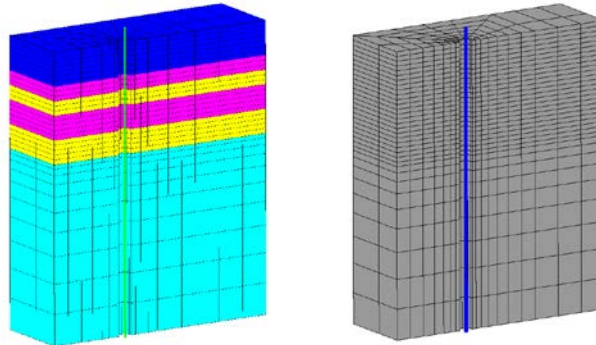


Fig. 2 - 3D finite element model and FE mesh created using GiD

For the purpose of creating the model, GiD, provides tools to choose appropriate geometries for each soil layer. With regard to available element types in OpenSees, element *SSPbrick* is used in this model. The *SSPbrick* element is an eight-node hexahedral element that uses physically stabilized single-point integration. The size of the elements is also considered in the model based on proximity of elements to the shaft and ground surface. As shown in 7(b), soil elements become smaller as they are closer to the surface and shaft.

There are various multi-dimensional soil constitutive models available in OpenSees. In this study, the elasto-plastic constitutive model proposed by Yang et al. (2003)[7], and here referred as *PressureIndependentMultiYield* (PIMY) material, is used to model the clay response. Similarly for sands, a pressure dependent model referred as *PressuredependentMultiYield* (PDMY) material is used in OpenSees. The main parameters required to define the sand and clay materials in OpenSees are presented in Table 4. Details on how to estimate the soil parameters for this model are discussed in [1].

Table 4 Soil properties used to define materials in OpenSees

Layer	Material model	Saturated mass density	Shear Modulus (MPa)	Bulk Modulus (MPa)	Peak Shear Strain	Friction angle	Cohesion (KPa)
First	PIMY*	1.841	3	9	0.0515	0	62.2
Second	PIMY	1.842	6	54	0.0515	0	62.2
Third	PDMY	2.082	100	220	0.031	40	0
Fourth	PIMY	1.842	6	54	0.0515	0	62.2
Fifth	PDMY	2.082	100	220	0.031	40	0
Sixth	PIMY	1.762	22	198	0.0495	0	167.7

After generating the soil domain, the shaft is added to the model using nonlinear beam elements. Note that half-sections are needed due to symmetry. Using beam elements to define the shaft creates the need to use appropriate contact elements between the shaft and soil; such that the shaft and soil movements are compatible. For this purpose, a beam-solid contact element is employed to simulate the interaction between soil and shaft. The contact elements are developed and implemented in OpenSees by Petek (2006) [8] and it is here referred as element *BeamContact3D*.



3-D analyses of shafts are performed in three steps including self-weight, axial load on the shaft and lateral displacement at the top of the shaft. As presented in Table 1, and for the particular case under study, the effective unit weight of the layers referred as cohesive, sand and Blue Gray clay are 8.26, 10.62 and 7.48 KN/m<sup>3</sup>, respectively.

After applying gravity, axial loading starts by increasing the load at the top of the shaft. Since the main concern in this study is with lateral loading, the estimated shaft weight, equal to 500 KN, is applied as a concentrated axial load on the shaft. Finally, lateral displacements are gradually imposed to the top of the shaft. As an example Figure 8 displays deflection, shear force and bending moment versus depth for section CNIR as calculated by OpenSees using 3D models.

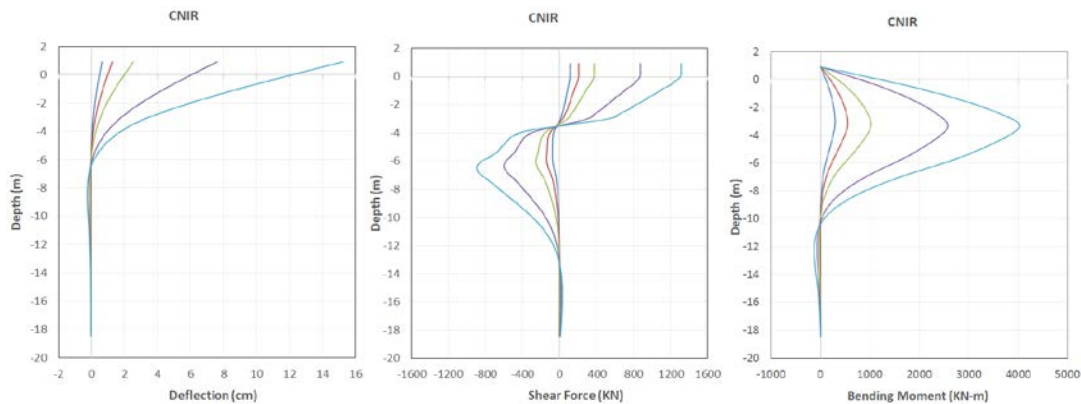


Fig. 8 - 3D OpenSees model. Deflection, shear force and bending moment versus depth at selected imposed displacements at the top of the shaft for CNIR section

## 7.0 Comparison of the 1-D Model to the 3-D Model

The response of laterally loaded shafts obtained from 1-D conventional models and the 3-D finite element models are compared in the terms of deflection, shear force and bending moment versus depth. As shown in Figure 9 to Figure 11, the response obtained using 1-D and 3-D models are in reasonable agreement. Figure 9 shows comparisons of deflection versus depth for all sections using both methods. The results show that both approaches result in very similar deflection profiles. Shear forces along the shafts are depicted in Figure 10. It is noticed that for small lateral displacements, the maximum absolute shear force for all sections obtained from 1-D conventional models is higher than that obtained using 3-D finite element models. For larger imposed displacements, however, the 3-D models show higher values for maximum absolute shear force. The same trend is observed in Figure 11 where the bending moment profile for different shafts is depicted using both approaches.

Table 5 compares maximum absolute shear force for different sections and imposed displacement based on results from both methods. In Table 6, maximum bending moment versus depth is presented and the results obtained from different methods are compared together. Take MIR for example, the ratios of applied lateral loads from the 1-D model over those from the 3-D model were 1.08, 1.07, 1.01, 0.99 and 0.91 with the imposed head displacements of 0.6, 1.3, 2.5, 7.6, and 15.2 cm, respectively; and the ratios of maximum bending moments were 0.97, 0.97, 1.0, 1.1, and 1.0, respectively.

This study confirms that results obtained from 1-D conventional and 3-D finite element approaches are similar. Generally speaking, for small lateral loading the 1-D conventional models generate higher response absolute shear and moment as compared to the 3-D finite element models. As lateral loading increases, the 3-D models produce a greater absolute shear and bending moment.

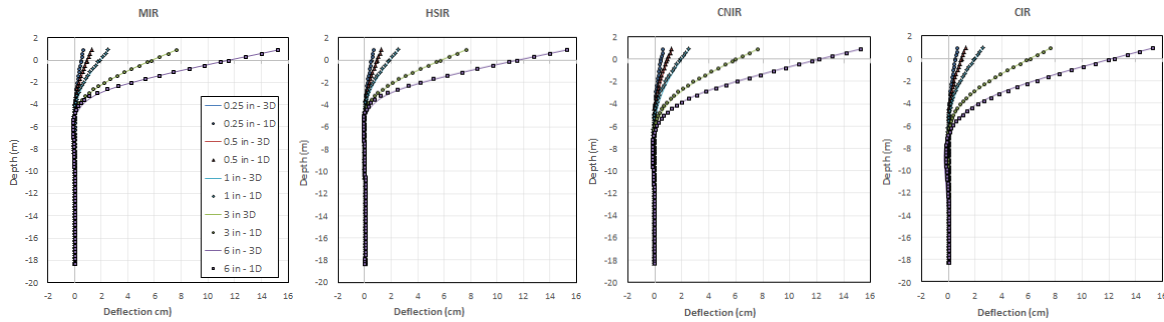


Fig. 9 - Comparison between 1D and 3D models - deflection versus depth at different displacements at the top of the shaft for each section

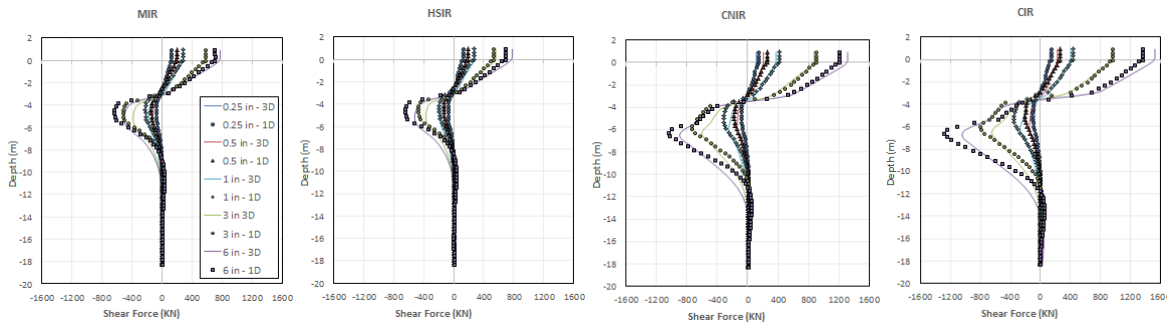


Fig. 10 - Comparison between 1D and 3D models – shear force versus depth at different displacements at the top of the shaft for each section

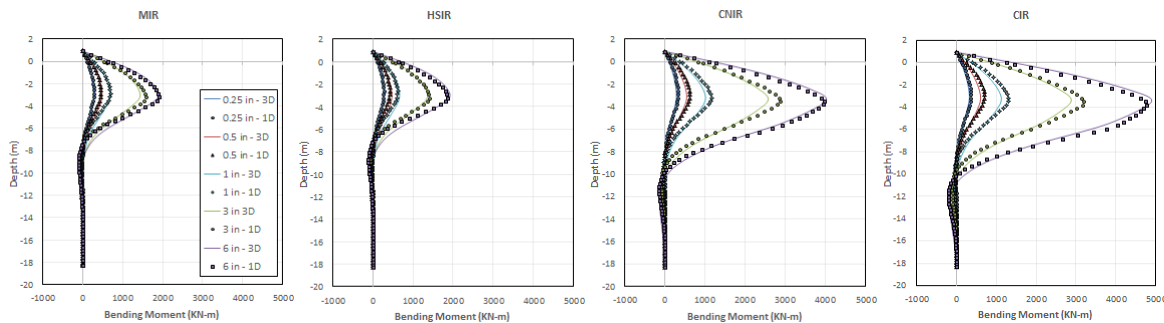


Fig. 11 - Comparison between 1D and 3D models - Bending moment versus depth at different displacements at the top of the shaft for each section

## 8.0 Conclusion

In this study, two different modeling approaches including a 1-D conventional finite element and a 3-D finite element approach have been used to evaluate the response of laterally loaded shafts. The OpenSees numerical platform was used for all simulations. In order to compare the performance of shafts with and without casing, four different sections, including MIR, HSIR, CNIR and CIR were defined in OpenSees and a methodology to extract the moment curvature relationship for the shafts was described. A procedure to develop 1-D conventional shaft models and a 3-D Finite element model in OpenSees was described. Results of lateral loading obtained by imposing displacements at the top of the free-head shafts using different methods were presented in corresponding sections.



Table 5 Comparison of 1D and 3D shear forces (in kN) induced by 0.6, 1.3, 2.5, 7.6, and 15.2 cm deflection at the top

Section	Analysis	0.6cm	1.3cm	2.5cm	7.6cm	15.2cm
<b>MIR</b>	1D	121	204	290	576	702
	3D	112	190	287	582	775
	1D/3D	<b>108%</b>	<b>107%</b>	<b>101%</b>	<b>99%</b>	<b>91%</b>
<b>HSIR</b>	1D	119	192	268	531	690
	3D	110	189	280	562	780
	1D/3D	<b>108%</b>	<b>102%</b>	<b>96%</b>	<b>94%</b>	<b>88%</b>
<b>CNIR</b>	1D	134	250	411	894	1193
	3D	114	208	374	874	1314
	1D/3D	<b>117%</b>	<b>120%</b>	<b>110%</b>	<b>102%</b>	<b>91%</b>
<b>CIR</b>	1D	146	272	450	972	1371
	3D	124	224	403	949	1523
	1D/3D	<b>118%</b>	<b>121%</b>	<b>112%</b>	<b>102%</b>	<b>90%</b>

Table 6 Comparison of 1D and 3D maximum bending moment (in kN-m) induced by 0.6, 1.3, 2.5, 7.6, and 15.2 cm deflection at the top

Section	Analysis	0.6cm	1.3cm	2.5cm	7.6cm	15.2cm
<b>MIR</b>	1D	277	467	697	1578	1914
	3D	285	484	693	1436	1905
	1D/3D	<b>97%</b>	<b>97%</b>	<b>100%</b>	<b>110%</b>	<b>100%</b>
<b>HSIR</b>	1D	271	429	623	1402	1866
	3D	280	477	670	1366	1925
	1D/3D	<b>97%</b>	<b>90%</b>	<b>93%</b>	<b>103%</b>	<b>97%</b>
<b>CNIR</b>	1D	320	629	1161	2859	3954
	3D	293	548	1019	2570	4016
	1D/3D	<b>109%</b>	<b>115%</b>	<b>114%</b>	<b>111%</b>	<b>98%</b>
<b>CIR</b>	1D	363	710	1315	3191	4766
	3D	328	611	1131	2876	4892
	1D/3D	<b>110%</b>	<b>116%</b>	<b>116%</b>	<b>111%</b>	<b>97%</b>



The ultimate lateral resistance of the test shafts were predicted roughly as 745, 743, 1289 and 1546 kN for shafts MIR, HSIR, CNIR, and CIR, respectively, indicating that using casing around the shaft of MIR added 107% extra lateral strength to shaft CIR. In addition, using casing without the internal reinforcement (CNIR) increased the lateral resistance of the shaft (MIR) by 73%. The results indicate that for sections with casing the depth of maximum rotation is deeper than the sections without casing. Lateral responses with different imposed displacements were compared between the test shafts. This study revealed that although cased shafts showed an increase in performance at very low deflections, the advantage of using casing becomes more significant for large deformations. Therefore, if a shaft is subjected to a large deformation such as in the case of liquefaction or in slickensided (pre-sheared) soil deposits, casing is a reasonable option comparing to the conventional concrete shafts. For the 3-D finite element models, results of lateral loading obtained by imposing displacements at the top of the free-head shafts were presented. The lateral responses in terms of deflection, shear force and bending moment profile obtained from 3-D models agreed well with the lateral responses from 1-D models

## 9.0 References

- [1] Stuedlein, AW, Q Li, P Arduino, and A Ganji (2015): Behavior of Drilled Shafts with High Strength Reinforcement and Casing. *Final Report* PACTRANS, USDOT University Transportation Center for Federal Region 10, University of Washington, Seattle, WA 98195.
- [2] Kulhawy, FH (1991). Drilled shaft foundations. *Foundation engineering handbook*, 2nd Ed., H. Y. Fang, ed., Van Nostrand-Reinhold, New York.
- [3] Reese, LC, and O'Neill, MW (1988). Drilled shafts: Construction procedures and design methods. *Pub. No. FHWA-HI-88-042*, U.S. Dept. of Transportation, Washington, D.C., 564–564.
- [4] Boulanger, RW, CJ Curras, BL Kutter, DW Wilson, and A Abghari. 1999. “Seismic soil-pile-structure interaction experiments and analyses.” *Journal of Geotechnical and Geoenvironmental Engineering*, ASCE, 125(9):750–759.
- [5] Matlock, H (1970). Correlations for Design of Laterally Loaded Piles in Soft Clay. *Proc., 2nd Annual Offshore Technology Conf.*, OTC 1204, Houston, Vol. 1, 577-594.
- [6] American Petroleum Institute (API). (1993). Recommended Practice for Planning, Designing and Constructing Fixed Offshore Platforms-Working Stress Design. *20th Ed., API RP2A-WSD*, Washington, D.C.
- [7] Yang, Z, A Elgamal and E Parra. 2003. “Computational Model for Cyclic Mobility and Associated Shear Deformation.” *Journal of Geotechnical and Geoenvironmental Engineering*, ASCE, 129(12), 1119-1127.
- [8] Petek, KA 2006. “Development and Application of Mixed Beam–Solid Models for Analysis of Soil-Pile Interaction Problems” *PhD Thesis, University of Washington*.